

# THE PECULIARITIES OF THE INTERACTION OF PHOBOS WITH THE SOLAR WIND ARE EVIDENCE OF THE PHOBOS MAGNETIC OBSTACLE (FROM PHOBOS-2 DATA)

V.G. Mordovskaya<sup>1</sup>, V.N. Oraevsky<sup>1</sup>, and V.A. Styashkin<sup>1</sup>

<sup>1</sup>*Institute of Terrestrial Magnetism, Ionosphere, and Radiowave Propagation (IZMIRAN), Troitsk, Moscow region, 142190 Russia, mail: valen@izmiran.rssi.ru*

## ABSTRACT

Using magnetic field and plasma data acquired during *Phobos-2* mission in regions which have not been explored before, we study the solar wind interaction with Phobos. The draping magnetic field of the solar wind around Phobos appears at distances of 200–300 km from the Phobos day-side due to a density and magnetic field pile up in front of the Phobos obstacle. The nature of the interaction and the magnetic field signatures observed are consistent with the ratio of the proton skin depth to the actual size of the Phobos obstacle to the solar wind. Phobos deflects the flow of the solar wind and the subsolar stand-off distance of the deflection is about 16–17 Phobos radii. Source with equivalent magnetic moment  $M' \simeq 10^{15}$  A·m<sup>2</sup> in Phobos leads to the development of such an obstacle to solar wind flow around Phobos. These data give a lesson for the study of the interaction of the small, magnetized object with solar wind.

## INTRODUCTION

The last planetary explorations have witnessed an increase of importance of investigations of small bodies of the Solar System because their substance may carry the information on an origin and evolution of Solar system. Interplanetary spacecraft have passed near several asteroidal bodies, i.e., Gaspra (20 km, 11 km), Ida (56 km, 21 km), Braille (1 km, 2.2 km), Eros (14 km, 34 km), and Martian moons Phobos (9.5 km, 13.5 km) and Deimos (5.5 km, 7.5 km). Within the parentheses given are the shortest and longest sizes of the bodies.

Galileo data showed the existence of magnetic field rotations near asteroids Gaspra at the closest approach distance 1600 km and Ida at 2700 km which have been interpreted as signatures of the solar wind interaction with the asteroids (Kivelson et al., 1993, 1995). Blanco-Cano et al. (2002) from own simulation results led to conclusion that the perturbation near Gaspra was not generated by the interaction of the solar wind with a magnetized asteroid and the signature observed near Ida was not generated by the interaction with the asteroid.

A 1 to 2 nT increase in the magnetic field perturbation at the distance 28 km from Braille was attributed by Richter et al. (2001) to a direct measurement of Braille magnetic field.

The solar wind interaction with the asteroid 433 Eros was investigated by the use of magnetometer data from the Near-Shoemaker spacecraft having circular orbits with radii of 200 km, 100 km, 50 km, and 35 km (Anderson and Acuna, 2003). No signature of an intrinsic asteroidal magnetic field was detected for Eros. Any draping or compressional signature associated with Eros was absent. Eros and Martian moons, Phobos and Deimos, have the same order of the ratio of the ion gyroradius and the ion skin depth to the body size. The magnetic field signatures of their interaction with the solar wind plasma have to be similar

if the moons can be considered as obstacles having the size of body.

However, the analysis of the magnetic field and plasma data aboard the Mars-5 spacecraft indicated that the Deimos obstacle to the solar wind is about 100 km (Bogdanov, 1977). It is much larger than the Deimos size.

The trajectory of *Phobos-2* provided the collection of data in regions which are appropriate for an investigation of interaction of Phobos with the solar wind and have not been explored before. The study of the interaction of Phobos with the solar wind plasma indicated that the day-side obstacle of Phobos to the solar wind is over 150 km. A sharp rise in the regular part of the magnetic field was observed on the circular orbits near Phobos at distances of 180–250 km from its center when Phobos was in the unperturbed solar wind (Yeroshenko, 2000).

Analyzing the data acquired aboard *Phobos-2*, Mordovskaya et al. (2001, 2002) gave evidence that Phobos has its own magnetic field and its magnetic moment is  $M' \simeq 10^{15}$  A·m<sup>2</sup>. The magnetic moment  $M'$  was estimated from pressure balance for the solar wind and the Phobos magnetic field measured at the magnetopause. The peculiarity of the rotation of the magnetized Phobos around Mars leads to the magnetic field signatures, which, especially the direction, are phase locked with Phobos rotation rate. Such magnetic field signatures were observed on circular orbit of the *Phobos-2* spacecraft (Mordovskaya et al., 2002).

In the present paper, we investigate the magnetic field enhancement observed near the dayside of Phobos in order to show that it is the kinetic theory that should be used when studying the solar wind interaction with a small magnetized bodies. We consider a density and magnetic field pile up in front of Phobos to illustrate that the magnetic field signatures observed are consistent with the ratio of the proton skin depth to the actual size of the Phobos obstacle to the solar wind. The occurrence or the absence of the shock-like structures ahead of the Phobos magnetopause correlates with behaviour of this ratio. In addition, we demonstrate how the solar wind is stopped and deflected away from Phobos by a magnetic barrier, which is compressed or expands depending on the solar wind ram pressure variations.

## THE MORPHOLOGY OF THE MAGNETIC FIELD SIGNATURES NEAR PHOBOS ON CIRCULAR ORBITS FROM MARCH 22 UNTIL MARCH 26, 1989

### Data Set

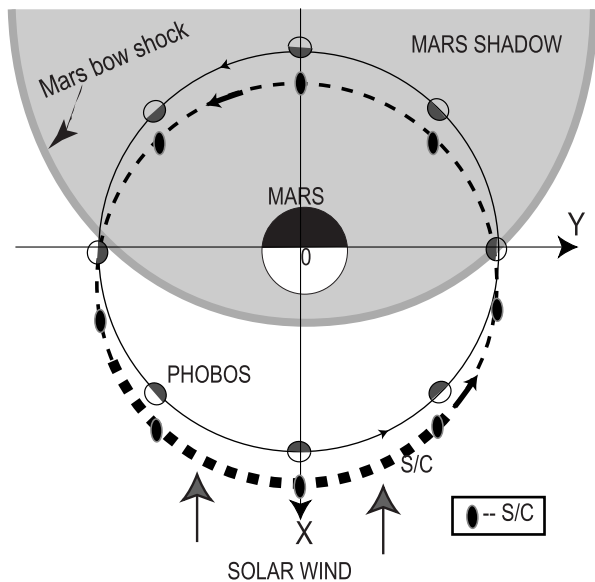


**Fig. 1.** View of the location of the *Phobos-2* and Phobos on March 22–26, 1989. Plot by line composed of small squares shows the segment of the S/C trajectory where the field enhancements were observed.

Vector measurements of the ambient magnetic field during *Phobos-2* mission were acquired by two magnetometers, FGMM and MAGMA (Riedler et al., 1989). Both instruments had a dynamic range of 100 nT and data were transmitted every 1.5, 2.5, 45, and 600 s, depending on the telemetry mode of the spacecraft. From March 22, 1989, to March 26, 1989, at each orbit around Mars, both *Phobos-2* spacecraft and the Mars satellite Phobos were inside the solar wind and within the Martian magnetosphere during 3.8 h. The spacecraft was located permanently in a vicinity of Phobos at this time and the distances between them were 180–400 km. A description of the spacecraft flight profile is given by Kolyuka et al. (1991). Figure 1 displays a sketch of the position of the *Phobos-2* and Phobos in the projection onto the Mars ecliptic plane  $XoY$  on March 22–26, 1989. The  $X$ -axis points to the Sun; the  $X$ - $Y$  plane coincides with the orbital plane of Mars; the  $Y$ -axis points in opposite direction of the Mars orbital velocity; the  $Z$ -axis is perpendicular to  $X$  and  $Y$ . The line composed of small squares allocates the part of the spacecraft trajectory on the circular orbit around Mars where the magnetic field enhancements were observed.

The morphology of the magnetic field signatures caused by the interaction of the Phobos magnetic field with the solar wind plasma and observed during the time interval of March 22–26, 1989 are presented in Figs. 2–4. The top panels of Figs. 2–4 present the segment of the spacecraft trajectory in the projection onto the Mars ecliptic plane  $XoY$  where these magnetic fields were acquired to demonstrate that the magnetic field enhancements in the regular part are not associated with Mars. With this aim, we indicate the location of the Mars bow shock deduced from the *Phobos-2* data and marked by the solid line in Fig. 1. The distance from the dayside surface of Mars to the position of the Mars shock is less than 400–1000 km. Studying the *Phobos-2* data, Schwingsenschuh et al., (1992) noted that the dependence of the bow shock position in the subsolar region on the solar wind dynamic pressure is weak. Really, over up month since February over March 1989 the spacecraft crossed the Mars bow shocks at  $X \approx 0$ ,  $Y = +9600$  and  $X \approx 0$ ,  $Y = -9600$  km. The position of the Mars bow shock crossing was the same during March 22–26, 1989. This location of the Mars bow shock was confirmed by a large database of bow shock crossings by the MGS spacecraft (Vignes et al., 2000; Luhmann et al., 2002). So the magnetic field enhancement in the regular part can not be really attributed to the Mars. The S/C crossed a stationary slowly moving structure, which approached to and then moved away from the S/C accordingly with the scheme of the S/C flight.

The plot of the distance  $R_x$  between Phobos and the spacecraft versus the time of the observation is represented in the bottom panels of Figs. 2–4 to illustrate that the magnetic field disturbances are really associated with Phobos. There is a clear correspondence between the disturbance of the magnetic field and the approaches of the spacecraft to Phobos. The magnetic field disturbances are associated with the solar wind interaction with Phobos. Below, the signs of the magnetic field components ( $B_{sx}$ ,  $B_{sy}$ ,  $B_{sz}$ ) of the undisturbed solar wind are presented to indicate an association of the phenomenon with the directions of the interplanetary magnetic field.

The plot of the magnitude of the magnetic field ( $B$ ) versus the time in the middle panels of Figs. 2–4. An absence of data for some time intervals leads to the fragmentary plot. The three components of the measured magnetic field are displayed in (Delva et al., 1994; Yeroshenko, 2000). In Figs. 2–4, the magnitude of the observed magnetic field is marked by the solar wind parameters acquired by *TAUS* device) ( $V_s$ –the solar wind velocity in km/sec,  $N_s$ –the solar wind density in  $\text{cm}^{-3}$ ) to illustrate that the manifestation of the phenomenon depends on the solar wind parameters. The arrows mark the time when the parameters were acquired.

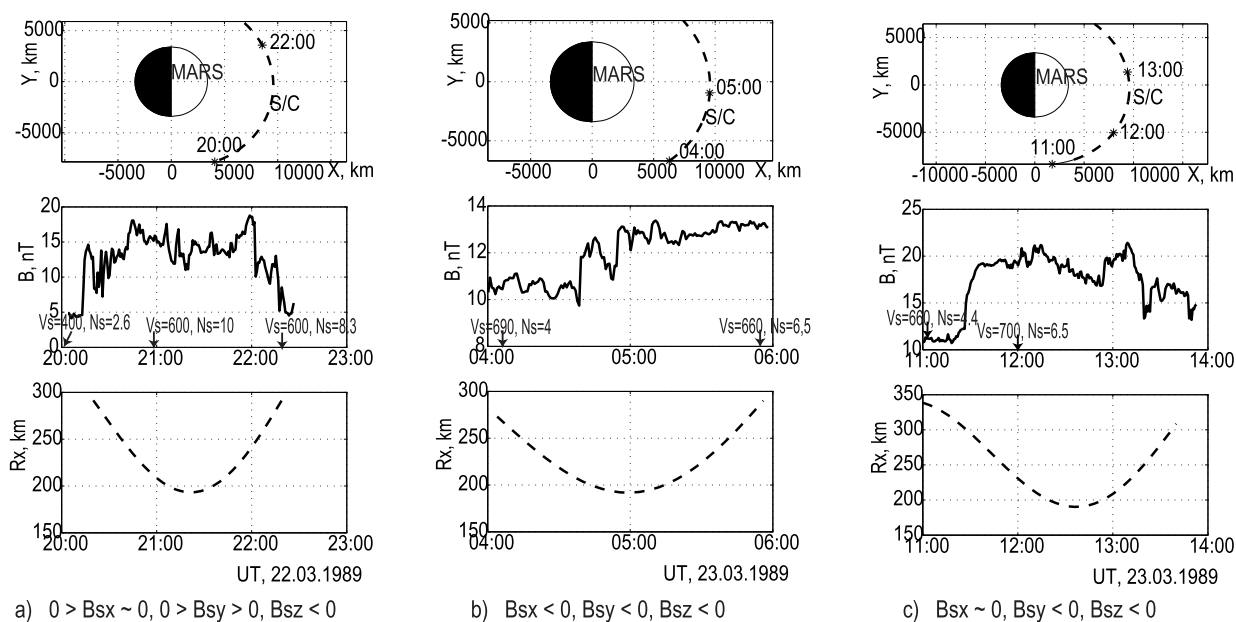


**Fig. 2.** On the top the plot of the magnetic field signatures and the appropriate spacecraft trajectories in the projection onto the Mars ecliptic plane  $XoY$ . The lower graphs correspond to the time history of spacecraft approaches to the dayside of Phobos inside the unperturbed solar wind. a) The data from 20:15 to 22:15 on March 22, 1989. b) The data from 04:00 to 06:00 on March 23, 1989. c) The data from 11:00 to 13:45 on March 23, 1989.

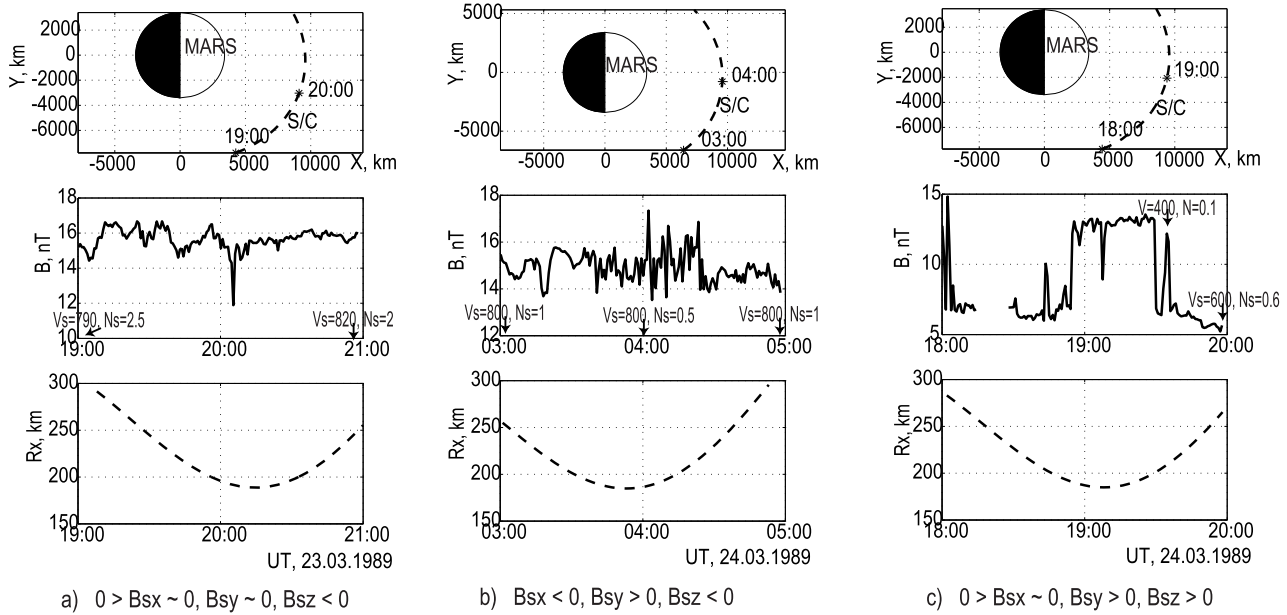


**Fig. 3.** Similar to Figure 2, except a) The data from 19:00 to 21:00 on March 23, 1989. b) The data from 03:00 to 05:00 on March 24, 1989. c) The data from 18:00 to 20:00 on March 24, 1989.

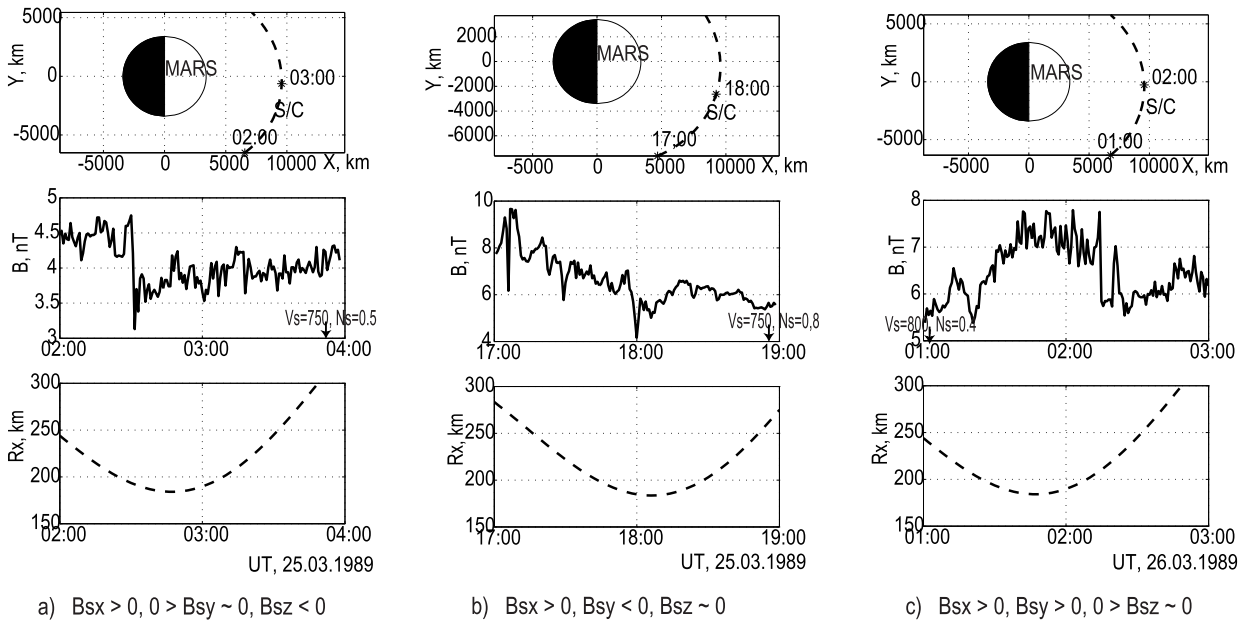


**Fig. 4.** Similar to Figure 2, except a) The data from 02:00 to 04:00 on March 25, 1989. b) The data from 17:00 to 19:00 on March 25, 1989. c) The data from 01:00 to 03:00 on March 26, 1989.

## Discussion

The small characteristic size of the Phobos obstacle to the solar wind have to give specific signatures of the solar wind-asteroid interaction. The typical free path for solar wind particles is much greater than the size of Phobos and the ion gyroradius for the solar wind plasma have the same order as the Phobos size. Therefore, a magneto-hydrodynamic approximation fails and it is necessary to use a kinetic theory to study the solar interaction with Phobos and other small bodies. In addition, it is worth noting that such MHD terms as “bow shock” and “subsolar magnetosheath” are inappropriate for description of the solar wind

interaction with a small magnetized asteroid.

The kinetic theory was used for description of interaction of spacecraft with magnetosphere plasma (Alpert et al., 1964). We can employ results inferred from the study. According to the kinetic theory, the density and magnetic field of the plasma pile up in front of the obstacle to the flow. The pile up becomes significant when the ion skin depth is comparable to the actual size of the obstacle. The same conclusion for the interaction of the solar wind with a magnetized asteroid was inferred by Blanco-Cano et al. (2002), which made the MHD simulation with ion kinetic effects.

Figures 2–4 give a lesson for the study of the solar wind interaction with a small, magnetized object. The magnetic field signatures observed near day-side of Phobos show the response of the solar wind to the Phobos obstacle. The draping magnetic field around Phobos appears at distances of 200–300 km from the Phobos day-side, the distance depends on the solar wind plasma parameters. The events displayed in Fig. 2 result from the interaction of the Phobos obstacle with the solar wind plasma having high density ( $N_s$ ) from  $3 \text{ cm}^{-3}$  up to  $12 \text{ cm}^{-3}$ . Figures 3 and 4 give the examples of the interaction in the plasma with lower density,  $N_s$  is between  $2 \text{ cm}^{-3}$  and  $0.4 \text{ cm}^{-3}$ . The velocity of the solar wind changes slightly during these observations. Therefore, the density of the solar wind plasma plays a significant role in formation of the size and shape of the draping and compressional region near the dayside of Phobos and around Phobos. The density and magnetic field of the solar wind plasma pile up in front of the obstacle that Phobos and its magnetic field represent to the solar wind. The pile up becomes significant when the proton skin depth is comparable with the actual size of the Phobos obstacle.

We can take the actual size of the Phobos obstacle from the paper by Mordovskaya et al. (2001) or estimate it from Figure 6 by calculating the size of region occupied by the planetary field of Phobos. This size is about 150–170 km and the relevant density is  $1.8\text{--}2.3 \text{ cm}^{-3}$ . Formation of a shock-like structure upstream of Phobos will take place for the solar wind plasma with density larger than  $1.8\text{--}2.3 \text{ cm}^{-3}$ . The magnetic field signatures in Fig. 2 demonstrate the shock-like structure upstream of Phobos and it is seen that in this case the draping of the field is stronger. Figures 3–4 show an absence of the shock-like structure ahead of Phobos magnetopause and the weak draping of the field around the Phobos obstacle because the plasma density was low. For other plasma densities observed, the ion scale length  $l_s$  is  $l_s=93 \text{ km}$  for  $N_s = 6 \text{ cm}^{-3}$ ;  $l_s = 130 \text{ km}$  for  $N_s = 3 \text{ cm}^{-3}$ ;  $l_s = 160 \text{ km}$  for  $N_s = 2 \text{ cm}^{-3}$ ;  $l_s = 294 \text{ km}$  for  $N_s = 0.6 \text{ cm}^{-3}$ . It is easily seen that the nature of the interaction displayed by the magnetic field signatures in Figs. 2–4 is related to the ion scale lengths. The presence or absence of a shock-like structure ahead of the Phobos magnetopause are consistent with the ratio of the proton skin depth to the actual size of the Phobos obstacle. Depending on this ratio, some ions and magnetic field line will pile up in front of the Phobos magnetic barrier, forming fanciful patterns of the density and magnetic field signatures. The field signatures observed are various and depend on the density of the solar wind flow.

It is worth dwell upon an additional feature of behavior of the plasma density and the magnetic field (see Figs. 3b and 3c). The density value decreases by a factor of 2 in Fig. 3b and by an order of magnitude with a closest approach to Phobos, the decrease indicates to the absence and lack of plasma, at least that of the solar wind, near regions adjacent to the Phobos magnetopause.

On March 24, 1989, the dynamic pressure of the solar wind begins to decrease. The density of the solar wind decreased down to  $0.5\text{--}1 \text{ cm}^{-3}$  during this period. When the speed  $V_s$  of the solar wind falls down to 600 km/s, it was possible to observe a remarkable event shown in Fig. 3c. During 18:43–19:41 on March 24, 1989 the magnetic field signature has a sharp rise with a characteristic “magnetopause-like” behavior demonstrating clear encounter with an intrinsic magnetic field of Phobos. The field magnitude increased by 80% with respect to the background level, while the plasma density value was, apparently, close to the lower threshold of sensitivity of the plasma detector. In detail, we consider the observation of the planetary magnetic field of Phobos in the next section.

The performed analysis of the magnetic field signatures observed near day-side of Phobos confirms that the nature of the interaction of Phobos with the solar wind is related to ion scale lengths and highlights the importance of studying the interaction of the solar wind with a small magnetized object using the kinetic theory. The small size of Phobos is the main cause of departures from a planet-like interaction with the solar wind. In agreement with the kinetic theory, the magnetic field of the solar wind drapes around the Phobos obstacle, the effect depends on the ratio of the proton skin depth to the actual size of the Phobos obstacle.

In Figs. 2-4, except for Fig. 3c, the magnetic field signatures are caused by the interaction of the solar wind with Phobos. On the other hand, Fig. 3c shows the direct measurements of the planetary magnetic field of Phobos.

### THE OBSERVATION OF THE PLANETARY MAGNETIC FIELD OF PHOBOS

The periapsis of the *Phobos-2* spacecraft was far from the dayside surface of Phobos, the smallest altitude is 170–180 km. We could directly probe the regions to see pure planetary magnetic field when the dynamic pressure of the solar wind dropped. There is a unique case of the manifestation of the Phobos intrinsic magnetic field during 18:43–19:41 on March 24, 1989 (Fig. 3c). In fig. 5 the three components of the measured magnetic field, velocity  $V$ , and density  $N$  of plasma for 18:00–20:00 of March 24, 1989 are displayed.

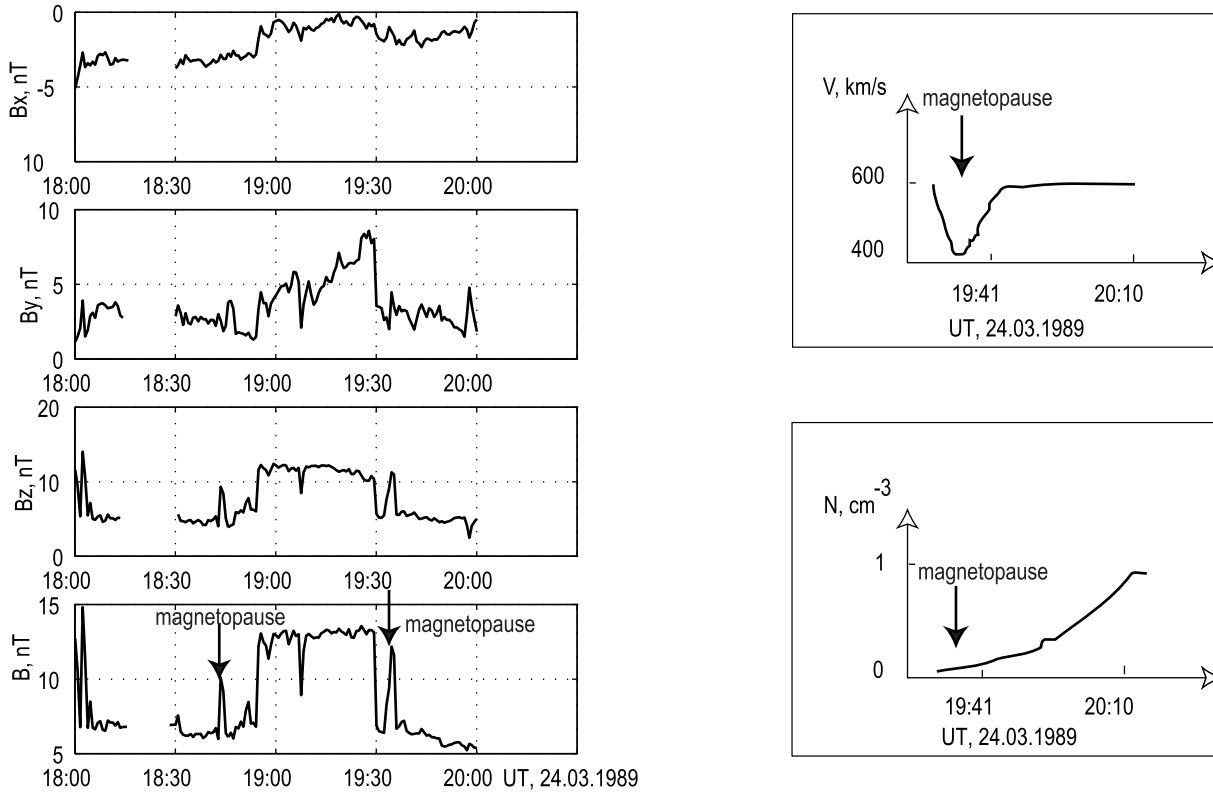


**Fig. 5.** Magnetic field and plasma data illustrating the encounter with a planetary magnetic field of Phobos as delineated by the arrows. **Left panels:** plot of the magnetic field components ( $B_x, B_y, B_z, B$ ) in nT. **Right panels:** plots of the plasma speed  $V$  in km/s and the plasma density  $N$  in  $\text{cm}^{-3}$

The data show the sharp boundary that clearly separates different plasma regions. The magnetic field enhancement ( $B$ ) is an almost rectangular pulse of a symmetrical shape with a characteristic “magnetopause-like” behavior. The encounter into the region occupied by the magnetic field of Phobos is indicated by a magnetopause crossing. The velocity signature says in favour of the existence of the magnetopause. Here we say about the magnetopause as a boundary separating the regions of the planetary magnetic field of Phobos and the solar wind plasma. The plasma density value was of order of  $0.1 \text{ cm}^{-3}$ , apparently, close to the lower threshold of sensitivity of the plasma detector. The absence of the solar wind plasma there gives a strong argument in favour of the existence of the region occupied by of the Phobos magnetic field.

The satellite seems to be in the subsolar point of the magnetosphere of Phobos near the magnetopause. The estimation of the magnetic moment of Phobos  $M'$  in the dipole approximation with help of the equation of pressure balance for the solar wind and the magnetic field of Phobos at the magnetopause and the experimental data was given by Mordovskaya et al. (2001):  $2N_s m_p V_s^2 = 1/8\pi (2M'/D^3)^2$ , where  $D$  is the distance from the center of the planet up to its subsolar point,  $N_s$  and  $V_s$  are the density and the speed of the solar wind, respectively,  $m_p$  is the proton mass. The measured values of the concentration and the



speed of the solar wind, which are used to estimate the magnetic moment  $M'$ , are  $N_s=0.17 \text{ cm}^{-3}$  and  $V_s=617 \text{ km/s}$ . The estimate obtained is  $M' \simeq 10^{15} \text{ A}\cdot\text{m}^2$ . It is a source with such magnetic moment in Phobos that can deflect the solar wind flow at the distance over 150–170 km from the dayside of Phobos.

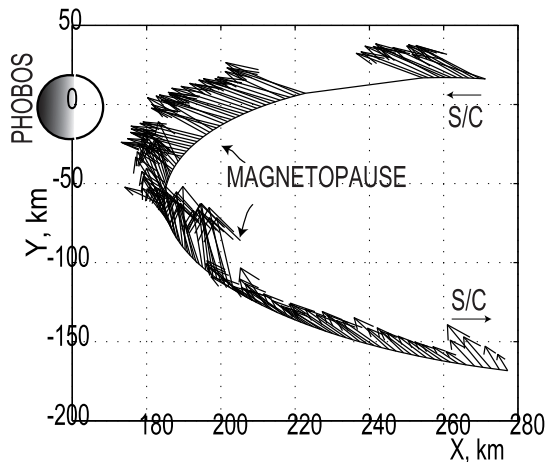


**Fig. 6.** Plot the amplitudes, the direction of vectors of the magnetic field  $B_x/B_y$  at 45-s intervals along the S/C trajectory in the Phobos centric coordinate system. The data are from 18:00 to 20:00 on March 24, 1989.

## CONCLUSION

In this study we have considered the solar wind interaction with Phobos using the magnetic field and plasma data from the *Phobos-2* mission during the closest fly-by on March 22–26, 1989. The magnetic field disturbances observed are correlated with the approaches of the spacecraft to Phobos. In the magnetic field signatures the manifestation of the interaction depends on the plasma parameters of the solar wind and are different for low and high plasma density. The draping magnetic field around Phobos appears at distances of 200–300 km from the Phobos day-side due to the density and magnetic field pile up in front of the Phobos obstacle. The nature of the interaction and the magnetic field signatures observed are consistent with the ratio of the proton skin depth to the actual size of the Phobos obstacle to the solar wind. On the other hand, the clear observation of the planetary magnetic field of Phobos is highly controlled by the  $B_{sz}$ ,  $B_{sy} > 0$  directions of the interplanetary magnetic field.

It was shown how Phobos deflects the flow of the solar wind. The subsolar stand-off distance of the deflection is about 16–17 Phobos radii. The planetary magnetic field of Phobos was clearly observed during 18:43 to 19:41 on March 24, 1989 at 170 km from the dayside of Phobos. The plasma and magnetic field data confirm this fact. By using the equation of pressure balance for the solar wind and the magnetic field of Phobos at the magnetopause, we calculated the equivalent magnetic moment  $M'$ , source of which in Phobos leads to the development of such an obstacle for solar wind flow around Phobos. In the dipole approximation, the magnetic moment of Phobos is  $M' \simeq 10^{15} \text{ A}\cdot\text{m}^2$ .

It is worth noting that the sizes of Phobos and an ion gyroradius of the interplanetary plasma have the same order of magnitude. This fact point out the Phobos magnetosphere to be a system having fundamental differences with that of the Earth.

The cause of density pile up is related to the actual size of the obstacle that Phobos and its magnetic field represent to the solar wind and highlights the importance of studying the interaction of the solar wind with a small magnetized object with the use of kinetic theory.

In conclusion, the magnetization of Phobos substance is 0.15 CGS. The third part of volume of Phobos should consist of a magnetic substance similar to a magnetite  $\text{Fe}_3\text{O}_4$  in order to obtain the given magnetization of Phobos. Since the density of Phobos is about  $2 \text{ g/cm}^3$ , we can suggest two explanations for the magnetization observed. First, Phobos is non-uniform and there exists an immense piece of a magnetic material within it. Second, Phobos consists of small pieces of a magnetic substance immersed into a non-magnetic low density material.

To give an additional grasp of the phenomenon, we display the *Phobos-2* encounter with the planetary magnetic field of Phobos with the help of magnetic field lines in Fig. 6. The amplitudes, the direction of vectors of the magnetic field  $B_x/B_y$ , and the S/C trajectory in the projection onto the Mars ecliptic plane  $XoY$  are given in the Phobos centric coordinate system. The field observed along the trajectory is represented by a scaled vector projection of  $\mathbf{B}$  originating from the position of the spacecraft at the corresponding times, the time interval between two consecutive measurements was 45 s. Analyzing the magnetic field direction near Phobos, we can determine with a great accuracy the boundary between completely open field lines of the solar wind and those with at least one end in Phobos. A dramatic change in the field line topology from 18:43 to 19:41 on March 24, 1989 indicates a transition from field lines with no connection to Phobos to field lines with at least one end in Phobos.

## ACKNOWLEDGEMENTS

We thank G. Kotova for providing some unpublished plasma data (experiment TAUS). V. Mordovskaya appreciates helpful communications and assistance of Ye. G. Yeroshenko.

## REFERENCES

- Acuna, M. H., J. E. P. Connerney, N. F. Ness, R. P. Lin, D. Mitchell, C. W. Carlson, J. McFadden, K.A. Anderson, H. Reme, C. Mazelle, D. Vignes, P. Wasilewski, and P. Clouter, Global distribution of crustal magnetism discovered by the Mars Global Surveyor MAG/ER Experiment, *Science*, **284**, pp. 790–793, 1999.
- Alpert, Ya. L., A. V. Gurevich, and L. P. Pitaevskii, Artificial satellites in a rarefied plasma, Moscow, Nauka, 1964.
- Anderson B. J., and M. Acuna, Observations of asteroid-solar wind interaction, submitted to *Adv. Space Res.*, 2003.
- Blanco-Cano, X., N. Omid, and C. T. Russell, Hybrid Simulations of solar wind interaction with magnetized asteroids: Comparison with Galileo observations near Gaspra and Ida, *J. Geophys. Res.*, **107**, N12, 2002.
- Delva, M., U. Nischelwitzer, K. Schwingenschuh, Despinning and tests of the Magma data in orbits around Mars, Report IWF-9407 of the Space Research Institute of Austrian Academy of Sciences
- Kivelson, M. G., L. F. Bargatze, K. K. Khurana, D. J. Southwood, R. J. Walker and P. J. Coleman Jr., Magnetic field signatures near Galileo's closest approach to Gaspra, *Science*, **261**, pp. 331–334, 1993.
- Kivelson, M. G., Z. Wang, S. Joy, K. K. Khurana, C. Polansky, D. J. Southwood, and R. J. Walker, Solar wind interaction with small bodies, 2, What can Galileo's detection of magnetic rotations tell us about Gaspra and Ida, *Adv. Space Sci.*, **16**(4), pp. 47–57, 1995.
- Kolyuka, YU. F., S. M. Kudryavtsev, V. P. Tarasov, V. P. Tikhonov, N. M. Ivanov, V. S. Polyakov, V. N. Potchukaev, O. V. Papkov, K. G. Sukhanov, E. L. Akim, V. A. Stepanians and R. R. Nasirov, International project Phobos. Experiment "Celestial Mechanics," *Planetary and Space Science*, **39**, pp.349–354, 1991.
- Luhmann, J. G., M. H. Acuna, M. Purucker, C. T. Russell, and J. G. Lyon, The martian magnetosheath: how Venus-like?, *Planetary and Space Science*, **50**, pp. 489–502, 2002.
- Mordovskaya, V. G., V. N. Oraevsky, V. A. Styashkin, and, J. Rustenbach, Experimental evidence of the Phobos magnetic field, *JETP Lett.*, **74**, pp. 293–297, 2001.
- Mordovskaya, V.G. and V.N. Oraevsky, In situ measurements of the Phobos magnetic field during the Phobos-2 mission, <http://xxx.lanl.gov>, *e-print arXiv:physics/0212073*, 2002
- Richter, I., D. E. Brinza, M. Cassel, K. H. Glassmeier, F. Kuhnke, G. Musmann, C. Othmer, K. Schwingenschuh, B.T. Tsurutani, First direct magnetic field measurements of an asteroidal magnetic field: DS1 at Braille, *Geophys. Res. Lett.*, **28**, p. 1913, 2001.
- Riedler, W., Möhlmann, D., Oraevsky, V. N., Schwingenschuh, K., Yeroshenko, Ye., Rustenbach, J., Aydogar, Oe., Berghofer, G., Lichtenegger, H., Delva, M., Schelch, G., Pisch, K., Fremuth, G., Steller, M., Arnold, H., Raditsch, T., Auster, U., Fornacon, K. H., Schenk, H. J., Michaelis, H., Mötschmann, U., Roatsch, T., Sauer, K., Schroedter, R., Kurths, J., Lenner, D., Linthe, J., Kobsev, V., Styashkin, V., Achache, J., Slavin, J., Luhmann, J. G., Russell, C. T., Magnetic fields near Mars: First results of the Phobos mission, *Nature*, **341**, p. 604, 1989.
- Schwingenschuh, K., W. Riedler, T.-L. Zhang et al., The martian magnetic field environment: induced or dominated by an intrinsic magnetic field?, *Adv. Space Res.*, **12**, pp. 213–219, 1992.
- Vignes, D., C. Mazelle, H. Reme, M. H. Acuna, J. E. P. Connerney, R. P. Lin, D. L. Mitchell, P. Clouter, D. H. Grider, N. F. Ness, The solar wind interaction with Mars: Locations and shapes of the bow shock and magnetic pile-up boundary from the observations of the MAG/ER Experiment onboard Mars Global Surveyor, *Geophys. Res. Lett.*, **27**, pp. 49–52, 2000.
- Yeroshenko, Ye. G., Interaction of the Solar Wind and Martian Magnetosphere with the Dust Disc of Phobos, *Cosmic Research*, **38**, pp. 119–130, 2000.